

# Bioinspired Flexible and Tough Layered Peptide Crystals

Lihl Adler-Abramovich,\* Zohar A. Arnon, XiaoMeng Sui, Ido Azuri, Hadar Cohen, Oded Hod, Leor Kronik, Linda J. W. Shimon, H. Daniel Wagner, and Ehud Gazit\*

One major challenge of functional material fabrication is combining flexibility, strength, and toughness. In several biological and artificial systems, these desired mechanical properties are achieved by hierarchical architectures and various forms of anisotropy, as found in bones and nacre. Here, it is reported that crystals of N-capped diphenylalanine, one of the most studied self-assembling systems in nanotechnology, exhibit well-ordered packing and diffraction of sub-Å resolution, yet display an exceptionally flexible nature. To explore this flexibility, the mechanical properties of individual crystals are evaluated, assisted by density functional theory calculations. High-resolution scanning electron microscopy reveals that the crystals are composed of layered self-assembled structures. The observed combination of strength, toughness, and flexibility can therefore be explained in terms of weak interactions between rigid layers. These crystals represent a novel class of self-assembled layered materials, which can be utilized for various technological applications, where a combination of usually contradictory mechanical properties is desired.

The development of materials exhibiting both high flexibility and high toughness often involves hierarchical designs, such as laminated organization—one of the simplest hierarchical forms. In several biological and artificial systems, these desired mechanical properties are obtained by the combination of hierarchical arrangements and structural anisotropy. The simplest form of anisotropy results from unidirectional organization of building blocks at the microscopic level, which can be further

combined into multilayer 3D structures as found in various biological organic–inorganic composites, including bones<sup>[1,2]</sup> and nacre<sup>[3]</sup> (Table 1). This multilayer approach has been technologically adopted in ancient alloys of superior mechanical properties, such as Damascus steel<sup>[4]</sup> and Japanese Katana (Table 1).<sup>[5]</sup> Unlike a homogeneous material, laminated structures with relatively weak interactions between the layers show high toughness by an interfacial crack deflection mechanism;<sup>[6]</sup> the weak interlayer interfaces may also contribute to a degree of flexibility in the case of forces applied perpendicularly to the plane of the layers, as was previously shown in crystalline systems.<sup>[7]</sup> In order to allow the formation of such lamination, combined with strength and toughness, it is of special interest to identify and employ simple building blocks by simple and conventional fabrication methods, with no

need for complicated procedures. Hence, molecular crystals may provide an attractive route to replace laminated materials in various technological applications. A central method for the production of molecular crystals is molecular self-assembly, in which molecules spontaneously arrange to form well-ordered structures.

Diphenylalanine (FF) is one of the most studied molecular crystal building blocks,<sup>[10]</sup> mainly due to the

Dr. L. Adler-Abramovich  
Department of Oral Biology  
The Goldschleger School of Dental Medicine  
Sackler Faculty of Medicine  
Tel Aviv University  
Tel Aviv 6997801, Israel  
E-mail: lihia@tauex.tau.ac.il


Z. A. Arnon, Dr. H. Cohen, Prof. E. Gazit  
Department of Molecular Microbiology and Biotechnology  
George S. Wise Faculty of Life Sciences  
Tel Aviv University  
Tel Aviv 6997801, Israel  
E-mail: ehudg@post.tau.ac.il

Dr. X. Sui, Dr. I. Azuri, Prof. L. Kronik, Prof. H. D. Wagner  
Department of Materials and Interfaces  
Weizmann Institute of Science  
Rehovot 7610001, Israel

Prof. O. Hod  
Department of Physical Chemistry  
School of Chemistry  
The Raymond and Beverly Sackler Faculty of Exact Sciences  
and The Sackler Center for Computational  
Molecular and Materials Science  
Tel Aviv University  
Tel Aviv 6997801, Israel

Dr. L. J. W. Shimon  
Department of Chemical Research Support  
Weizmann Institute of Science  
Rehovot 7610001, Israel

Prof. E. Gazit  
Department of Materials Science and Engineering, Iby and Aladar  
Fleischman Faculty of Engineering  
Tel Aviv University  
Tel Aviv 6997801, Israel

 The ORCID identification number(s) for the author(s) of this article can be found under <https://doi.org/10.1002/adma.201704551>.

DOI: 10.1002/adma.201704551

**Table 1.** Laminated materials.

Material	Significant components	Characteristics	Reference
Bone	Collagen and hydroxyapatite	Strong and flexible	[1]
Nacre	Elastic proteins and calcium carbonate	Tough	[3]
Damascus steel	Steel of altering carbon percentage	Tough and stiff	[4]
Japanese Katana	Steel of altering carbon percentage	Tough and stiff	[5]
Laminated armor	Unidirectionally oriented olefin polymer films	High impact resistance and high resistance to shattering	[8]
Polymeric laminates	Polycarbonate resin and interlayers of elastomeric resin	Efficient energy absorption	[9]

exceptional properties of the assembled structures, including piezoelectricity,<sup>[11]</sup> pyroelectricity,<sup>[12]</sup> semiconductivity,<sup>[13]</sup> and photoluminescence.<sup>[14]</sup> Some of the unique mechanical characteristics of FF assemblies were attributed to noncentrosymmetric crystalline organization at the microscopic level.<sup>[15]</sup> Interestingly, the FF dipeptide self-assembles into tubular structures with a Young's modulus of 19 GPa in its hydrated state,<sup>[16]</sup> comparable to human cortical bone.<sup>[17]</sup> A related N-capped dipeptide, *N*-(*t*-butoxycarbonyl)-L-Phe-L-Phe-COOH (Boc-FF), can associate into distinct nanoscale morphologies depending on variations in the assembly conditions, such as solvent composition or peptide concentration.<sup>[18]</sup> A direct set of measurements of the mechanical properties of the spherical Boc-FF structures, conducted using an atomic force microscope (AFM) diamond-tip cantilever, demonstrated a remarkable metallic-like Young's modulus.<sup>[19]</sup>

To comprehensively study the molecular interactions that facilitate the formation of ordered nanostructures by Boc-FF, we set out to crystallize the peptide and acquire single-crystal X-ray diffraction data. Boc-FF was dissolved to a final concentration of 5 mg mL<sup>-1</sup> in 50% ethanol and incubated at room temperature for crystallization. After ≈2 months, crystals were visibly ubiquitous inside the tube, with several nucleation sites on the solution-tube surface and numerous rod-shaped crystals propagating from each nucleation site.

To gain atomic resolution insights into the assembly process and the stability of the nanostructures, single-crystal X-ray diffraction analysis was performed to determine the molecular packing. The crystal structure was found to exhibit a monoclinic space group *C2* with two independent molecules per asymmetric unit (Figure 1a) for a total of eight molecules per unit cell (Figure 1b,c). Complete crystallographic details are given in Table S1 in the Supporting Information. The packing is facilitated by a network of aromatic interactions and hydrogen bonds. Surprisingly, unlike most molecular crystals, which form rigid structures, Boc-FF crystals demonstrate unique elastic flexibility (Figure 1d,e; Video S1, Supporting Information).

To further examine the structure of the crystals, samples were characterized by high-resolution scanning electron microscopy (HRSEM; Figure S1, Supporting Information). The microscopic analysis revealed that each individual crystal is composed of a stack of 2D sheets, resulting in a rod-shaped multilayer, with a nearly rectangular cross section (Figure 2a). We also observed an anisotropy of the crystal, as the rod is made of parallel continuous layers running through its longitudinal direction. Based on the correlation between the HRSEM

and X-ray structure, we could determine that the long axis of the crystal is always aligned with the *b* axis (*y* Cartesian direction), the other lamellar plane axis is *c* (*z* Cartesian direction), and the direction in which the layers are stacked is the projection of the *a* axis along the *x* Cartesian direction.

To explore the mechanical properties that mediate this remarkable anisotropy and flexibility, a set of tests were performed using bending and tensile manipulations. Due to the high flexibility of the crystal, the bending force is very small and traditional load cells cannot fulfill the task of force measurement with satisfactory resolution. Therefore, we used an AFM tip and a cantilever configuration (Figure 2b). The movement of the nanomanipulator perpendicular to the cantilever resulted in both deflection of the peptide rod and bending of the AFM cantilever. Provided that the spring constant of the cantilever is known, the deflection of the cantilever can be translated to a force. Here, an AFM cantilever with a spring constant of ≈3 N m<sup>-1</sup> was used to push the crystal rod at different positions along the longitudinal axis (*b* axis) for three to six times as presented in Table S2 in the Supporting Information. When the force is applied at an arbitrary position, the deflection of the free end of the crystal can be expressed as

$$\delta = \frac{Pl_1^2}{6EI}(3L - l_1) \quad (1)$$

where  $\delta$  is the crystal deflection at its edge,  $P$  is the bending force,  $E$  is the bending modulus,  $I$  is the second moment of inertia,  $L$  is the total length of the crystal, and  $l_1$  is the distance from the fixed end to the point where the force is applied.<sup>[20]</sup> Due to the anisotropic nature of the laminated structure, different bending properties are expected when the force is exerted in different directions, parallel or perpendicular to the layering basal plane. Following the bending test, the geometry of each sample was examined using HRSEM. Since all peptide crystals exhibited a nearly rectangular cross section, the expression of the moment of inertia of a perfect rectangular prism was used. The bending test results are summarized in Table S2 in the Supporting Information. Clearly, the crystal shows anisotropic mechanical stiffness, with average bending moduli of 15.9 ± 4.1 GPa in the *z* Cartesian direction (*c* axis, similar to human cortical bone, about 18 GPa) and 5.5 ± 1.2 GPa in the *x* direction (similar to Nylon 6, about 3 GPa), in correlation with the laminated structure of the crystal. As the *z* direction is within the lamellar plane, bending in the *z* direction means applying force in the lateral direction of the plane, while bending in the *x* direction means applying force in the direction of the

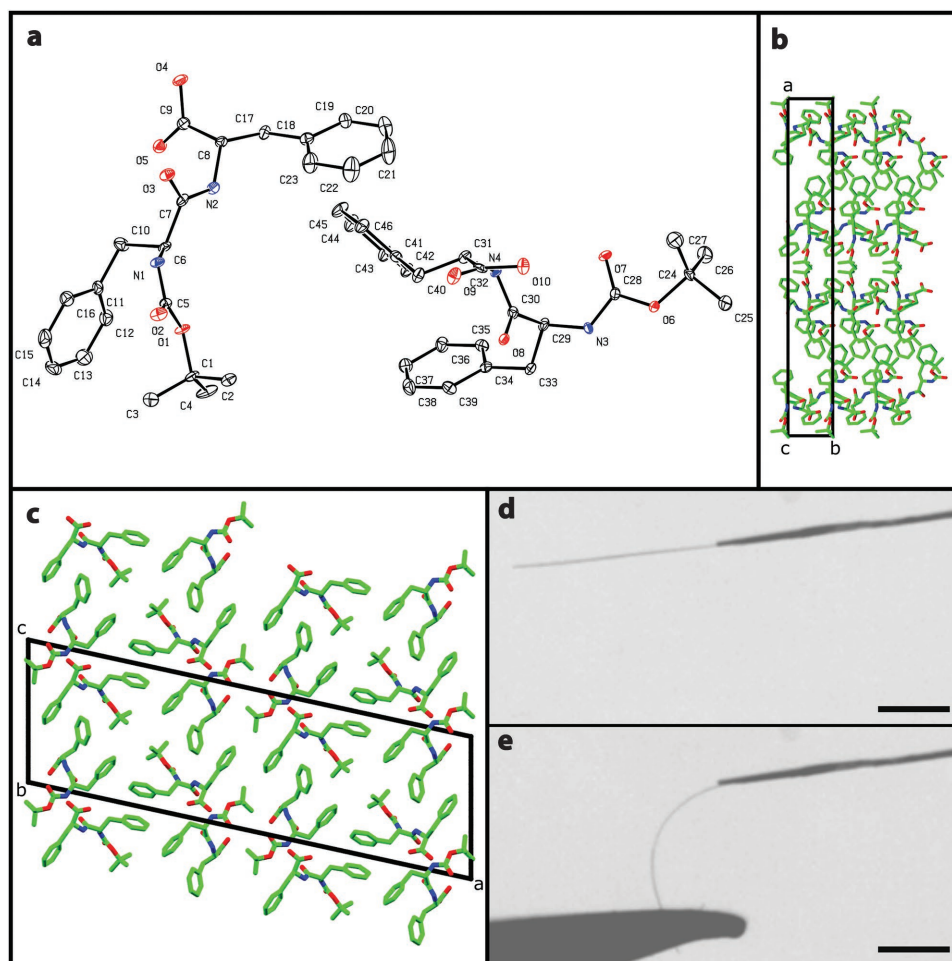


**Figure 1.** Crystal structure and mechanical flexibility of Boc-FF. a) Boc-FF ORTEP figure drawn with 50% probability ellipsoids, obtained via single-crystal X-ray structure determination at a resolution of 0.8 Å. Hydrogens have been omitted for clarity. b,c) Crystal packing down the *c* and *b* axes, respectively. For more information, see Table S1 in the Supporting Information. d,e) Demonstration of the extraordinary mechanical flexibility of the Boc-FF crystal using light microscopy. A single crystal rod is bent when force is applied using tweezers. The scale bar is 0.5 mm.

plane's normal vector (Figure 2c). It is important to note that no decrease in the modulus was observed upon repeated applications of force (Table S2, Supporting Information). Whereas within a single layer the Boc-FF molecules are closely packed, between the lamellae there are weak van der Waals interactions and hydrogen bonds. In-plane bending will therefore result in a higher modulus than out-of-plane bending. We also observed that in each direction of the same sample, pushing at different positions of the crystal ( $l_1$  in Figure 2b) yields similar moduli (Table S2, Supporting Information), which validates the method of modulus determination of the thin crystal rods by the AFM cantilever. When bending in the *z* direction of sample 2, we did not observe any deflection of the cantilever. This is due to the fact that the force exerted from the bending of the crystal, which was too thin in the *z* direction, was below the detection limit of the measurement device. Therefore, we avoided crystals that were too thin.

Additional tensile tests were performed using a tailor-made small-scale testing apparatus (Figure 2d). Following each test, the samples were examined using HRSEM for precise measurements of the specimen cross-sectional dimensions. The

tensile tests and the stress–strain curves for 11 samples are shown in Figure 2e,f. The results are summarized in Table S3 in the Supporting Information.

The outcome of a typical tensile test is often presented as a stress–strain curve. Stress is the force applied to the sample normalized by the cross-sectional area (units:  $\text{N m}^{-2}$ , or Pa), whereas strain is the displacement caused by the external force, normalized by the initial length of the sample ( $\text{m m}^{-1}$ , thus either no units or % if this is multiplied by 100). The stress–strain curves of the Boc-FF peptide specimens (Figure 2e) revealed an elastic behavior, contrary to other organic systems.<sup>[7]</sup> The average strain to failure of Boc-FF crystals was about 5%, while one exceptional specimen had a strain closer to 10%. The average strength and Young's modulus were 104 MPa and 3.1 GPa, respectively. Toward the end of the stress–strain curve, some specimens showed kinks, but the stress continued to rise before final failure (Figure 2f). The kinks sometimes occurred repeatedly, indicating that the rods fail gradually rather than abruptly. This fracture behavior was confirmed by video recording during the test (Video S2, Supporting Information) and postfailure HRSEM images of the samples following the

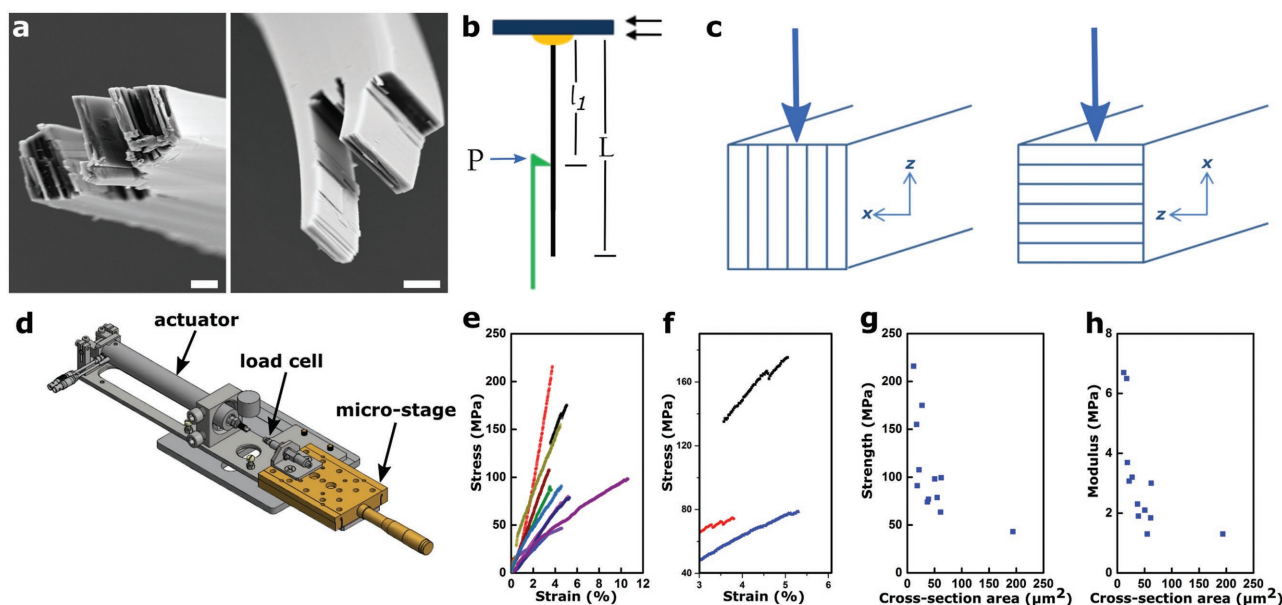


**Figure 2.** Mechanical measurements. a) HRSEM images of the laminated Boc-FF crystal (scale bars are 2  $\mu\text{m}$ ). b) Bending test experimental setup.  $P$  is the bending force,  $L$  is the total length of the crystal, and  $l_1$  is the distance from the fixed end to the point where the force is applied. c) Illustration of the laminated crystals relative to the testing direction. d) Tensile test experimental setup. e) Stress–strain curves of the tensile test normalized to the cross section of the sample and f) curves that present kinks before failure. g, h) The relationship between cross-sectional area and tensile strength or Young’s modulus, respectively.

tensile tests (Figure 2a). The HRSEM images clearly showed that the fracture surfaces were rough. The rods are made of parallel 2D layers, and the adhesion between two neighboring sheets is most likely not strong. Due to the weak van der Waals interactions and hydrogen bonds between the crystal layers, there is insufficient local stress sharing between them. Under stress, each layer of such a laminated specimen breaks at its own weakest point, leading to cracks zigzagging through the specimen bulk. This anisotropic fracture behavior is a direct manifestation of the layered structure of the crystal.

Interestingly, the tensile strength and Young’s modulus decreased as the cross-sectional area increased (Figure 2g,h). This has been previously observed for a number of micro- and nanofiber samples.<sup>[21]</sup> We believe that a larger cross section has

more weak interactions between layers, which do not contribute to the load sharing, resulting in lower strength and modulus of the bulk. The actual strength and modulus of a single layer are therefore expected to be much higher than the average measured values, as shown in the bending tests.

To further examine this hypothesis, we performed first-principles calculations for the structural and mechanical properties of the pristine Boc-FF molecular crystal using dispersion-corrected density functional theory (DFT) calculations (see “Density Functional Theory Calculations” in the “Methods” section in the Supporting Information). Importantly, this approach has been previously shown to be a reliable method for computing and predicting structural and mechanical properties of amino acid and peptide-based molecular crystals.<sup>[22,23]</sup> Lattice

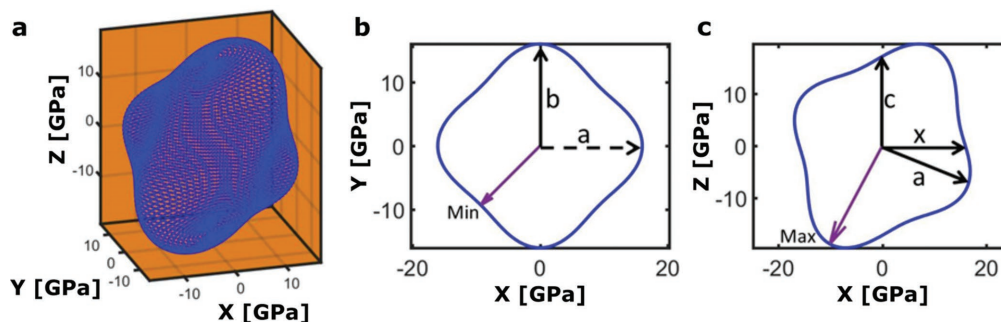


**Figure 3.** Computed rendering of Young’s modulus of Boc-FF single crystal. a) 3D surface, constructed by setting the distance from the origin to each point on the surface to the value of Young’s modulus in the direction of the vector pointing from the origin to that point. The axes are given in GPa and negative signs indicate the direction. b, c) 2D rendering of Young’s modulus projection on the  $x$ - $y$  and  $x$ - $z$  planes, respectively. The distance from the origin to each point on the line is the value of Young’s modulus in the direction of the vector pointing from the origin to that point. Purple arrows designate directions for minimum and maximum values of Young’s modulus for the crystal. The dashed arrow in panel (b) designates the projection of the lattice vector  $a$  on  $x$ . In all plots, the lattice vector  $c$  is aligned with the  $z$  axis,  $a$  is on the  $x$ - $z$  plane, and  $b$  is on the  $y$  axis.

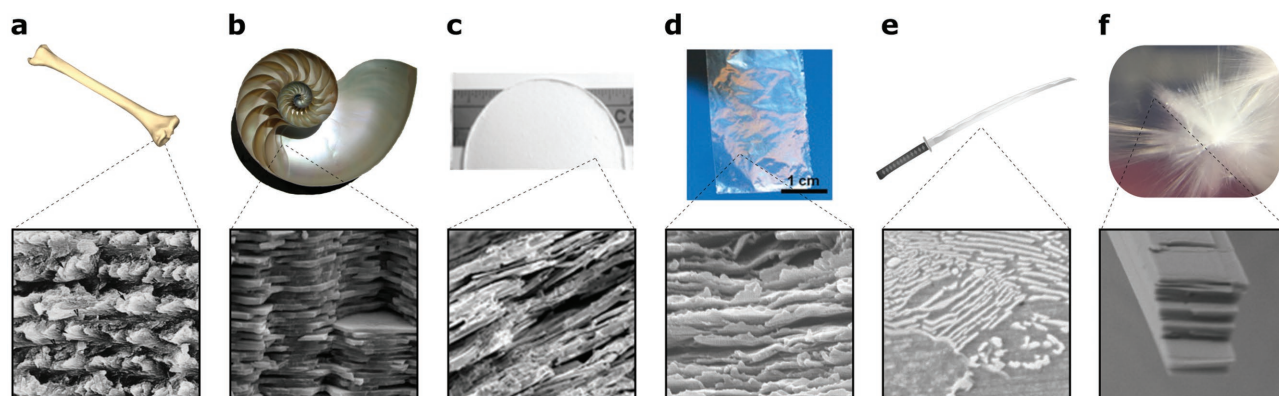


**Figure 4.** Lamination in various natural biological systems and manmade materials. a–f) Scanning electron microscopy images (lower panels) illustrating the lamination of each material (upper panels). a) Cortical bone.<sup>[1]</sup> b) Hexagonal platelets of calcium carbonate crystals in nacre.<sup>[3]</sup> c) Cross section of bone biomimetic composites.<sup>[25]</sup> d) Layered polymer nanocomposite film.<sup>[26]</sup> e) Microfolding of Japanese swords.<sup>[9]</sup> f) Boc-FF crystals growing from a mutual nucleation site.

parameters of the optimized crystal structure are given in Table S4 in the Supporting Information, showing good agreement between the experimental and computational values, thus validating the calculated mechanical properties.

Elastic constants were extracted from computed stress–strain curves<sup>[24]</sup> (Figure S2, Supporting Information) and used to calculate Young's moduli. Along the  $c/z$  direction, on which the layered nature of the structure has the least significant effect, the calculated Young's modulus is  $E_{c/z} = 17.2$  GPa, which is within experimental error margins of the measured value,  $15.9 \pm 4.1$  GPa. For the  $x$  and  $b/\gamma$  directions, the calculated values for the ideal crystal ( $E_x = 16.0$  GPa and  $E_{b/\gamma} = 15.9$  GPa) are indeed substantially larger than the measured values [5.5 GPa (bending) and 3.1 GPa (tensile)]. This is fully in line with the above hypothesis, namely that the large measured anisotropy in Young's modulus values is not an intrinsic property of the pristine single crystal, but rather is acquired by virtue of the layered structure. We note that a complete 3D rendering of the orientational dependence of Young's modulus (Figure 3) does reveal some anisotropy, from a minimum value of 13.0 GPa (in the  $x$ – $y$  plane) to a maximum value of 21.4 GPa (in the  $x$ – $z$  plane). Previous studies of amino acid crystals often found a significantly higher degree of anisotropy (e.g., for glycine- and alanine-based crystals), which has been associated with significant anisotropy in the direction of the hydrogen bond network in these solids.<sup>[23]</sup> For Boc-FF, a hydrogen bond analysis reveals five relevant hydrogen bonds, that is, with significant projection along the  $x$  and/or  $z$  axis, in each molecular dimer. Of those, detailed projection shows a contribution of  $\approx 60\%$  along the  $z$  axis and  $\approx 40\%$  along the  $x$  axis. The variation is relatively small, in agreement with the modest Young's modulus anisotropy.

The Boc-FF system thus provides a vivid example for the spontaneous assembly of remarkably simple building blocks into crystalline structures of laminated organization. In spite of the fact that comparable or even higher Young's moduli were calculated for FF derivatives, the mechanical anisotropy of the crystals described in this work results in notable flexibility, rarely observed in such ordered crystals. Beyond this very interesting phenomenon, this laminated system is very attractive

from the technological point of view. Layered structures are commonly found in the biological world (Figure 4a,b). Some notable cases include vertebrate bones and nacre, in which carbonated hydroxyapatite and calcium carbonate minerals, respectively, are organized in a lamellar manner. Lamination is also used in materials engineering. One such example is the production of laminated bone biomimetic composites of amyloids and hydroxyapatite<sup>[25]</sup> (Figure 4c). Another elegant approach in the organic world includes the engineering of polymeric systems to produce an ultrastrong and stiff layered polymer nanocomposite made of polyvinyl alcohol and montmorillonite<sup>[26]</sup> (Figure 4d). In addition, for centuries, lamination was an effective way to achieve toughness and flexibility of various alloys, including Damascus steel and Japanese Katana (Figure 4e). For these reasons, we suggest the Boc-FF system as an attractive candidate for biomedical engineering as a reinforcement for bone and bone substitutes, as well as a bioinspired composite material, similar to the application of graphene.

The newly described peptide system (Figure 4f) combines the remarkable advantage of lamination of a single component together with notable bottom-up self-assembly and unique physical properties of the FF system. FF dipeptides have been utilized for numerous applications, ranging from energy generation and storage<sup>[11]</sup> to prototypes of biomedical and bioengineering devices.<sup>[27]</sup> Hence, the stability, processability, and compatibility with standard manufacturing procedures make this family of building blocks especially attractive.

## Supporting Information

Supporting Information is available from the Wiley Online Library or from the author.

## Acknowledgements

L.A.-A., Z.A.A., and X.S. contributed equally to this work. This work was supported by the Israeli National Nanotechnology Initiative and Helmsley Charitable Trust (E.G.) and the European Research Council BISON project (E.G.). The authors thank members of the Gazit and

Adler-Abramovich groups as well as Dr. Asaf Azuri (Weizmann Institute) for helpful discussions. The authors would like to acknowledge support from the G.M.J. Schmidt Minerva Centre of Supramolecular Architectures at the Weizmann Institute. This research was also made possible in part by the generosity of the Harold Perlman family. H. Daniel Wagner is the recipient of the Livio Norzi Professorial Chair in Materials Science. The authors would also like to acknowledge Dr. Ifat Kaplan-Ashiri for help with electron microscopy analysis and Dr. Eyal Shimoni for help with the cryo-SEM characterization. O.H. acknowledges the Lise Meitner Minerva Center for Computational Quantum Chemistry and the Center for Nanoscience and Nanotechnology at Tel Aviv University for their generous financial support.

## Conflict of Interest

The authors declare no conflict of interest.

## Keywords

DFT calculations, flexible organic crystals, layered materials, mechanical properties, supramolecular biochemistry

Received: August 11, 2017

Revised: October 19, 2017

Published online: December 7, 2017

- [1] S. Weiner, W. Traub, H. D. Wagner, *J. Struct. Biol.* **1999**, 126, 241.
- [2] E. Seeman, P. D. Delmas, *N. Engl. J. Med.* **2006**, 21354, 2250.
- [3] F. Song, A. K. Soh, Y. L. Bai, *Biomaterials* **2003**, 24, 3623.
- [4] D. T. Peterson, H. H. Baker, J. D. Verhoeven, *Mater. Charact.* **1990**, 24, 355.
- [5] M. Yaso, T. Takaiwa, Y. Minagi, K. Kubota, S. Morito, T. Ohba, A. K. Das, in *ESOMAT 2009—8th Eur. Symp. on Martensitic Transformations*, EDP Sciences, Les Ulis, France **2009**, p. 7018.
- [6] D. Kovar, M. D. Thouless, J. W. Halloran, *J. Am. Ceram. Soc.* **1998**, 81, 1004.
- [7] a) P. Naumov, S. Chizhik, M. K. Panda, N. K. Nath, E. Boldyreva, *Chem. Rev.* **2015**, 115, 12440; b) G. R. Krishna, R. Devarapalli, G. Lal, C. M. Reddy, *J. Am. Chem. Soc.* **2016**, 138, 13561; c) M. K. Panda, S. Ghosh, N. Yasuda, T. Moriwaki, G. D. Mukherjee, C. M. Reddy, P. Naumov, *Nat. Chem.* **2015**, 7, 65; d) M. Owczarek, K. A. Hujsak, D. P. Ferris, A. Prokofjevs, I. Majerz, P. Szklarz, H. Zhang, A. A. Sarjeant, C. L. Stern, R. Jakubas, S. Hong, V. P. Dravid, J. F. Stoddart, *Nat. Commun.* **2016**, 7, 13108; e) M. K. Panda, K. Bhaskar Pal, G. Raj, R. Jana, T. Moriwaki, G. D. Mukherjee, B. Mukhopadhyay, P. Naumov, *Cryst. Growth Des.* **2017**, 17, 1759.
- [8] R. R. Holmes, *US4309487 A*, **1972**.
- [9] H. E. Littell Jr., *US4081581 A*, **1976**.
- [10] a) X. Yan, P. Zhu, J. Li, *Chem. Soc. Rev.* **2010**, 39, 1877; b) L. Adler-Abramovich, E. Gazit, *Chem. Soc. Rev.* **2014**, 43, 6881.
- [11] V. Nguyen, R. Zhu, K. Jenkins, R. Yang, Y. Jin, *Nat. Commun.* **2016**, 7, 13566.
- [12] A. Esin, I. Baturin, T. Nikitin, S. Vasilev, F. Salehli, V. Y. Shur, A. L. Kholkin, *Appl. Phys. Lett.* **2016**, 109, 142902.
- [13] B. Akdim, R. Pachter, R. R. Naik, *Appl. Phys. Lett.* **2015**, 106, 183707.
- [14] J. S. Lee, I. Yoon, J. Kim, H. Ihee, B. Kim, C. B. Park, *Angew. Chem.* **2011**, 123, 1196; *Angew. Chem., Int. Ed.* **2011**, 50, 1164.
- [15] A. Kholkin, N. Amdursky, I. Bdkin, E. Gazit, G. Rosenman, *ACS Nano* **2010**, 4, 610.
- [16] a) N. Kol, L. Adler-Abramovich, D. Barlam, R. Z. Shneck, E. Gazit, I. Rousso, *Nano Lett.* **2005**, 5, 1343; b) P. S. Zelenovskiy, V. V. Yuzhakov, S. G. Vasilev, A. L. Kholkin, V. Ya Shur, *IOP Conf. Ser. Mater. Sci. Eng.* **2017**, 256, 12012.
- [17] J. Y. Rho, R. B. Ashman, C. H. Turner, *J. Biomech.* **1993**, 26, 111.
- [18] A. Levin, T. O. Mason, L. Adler-Abramovich, A. K. Buell, G. Meisl, C. Galvagnion, Y. Bram, S. A. Stratford, C. M. Dobson, T. P. J. Knowles, E. Gazit, *Nat. Commun.* **2014**, 5, 5219.
- [19] L. Adler-Abramovich, N. Kol, I. Yanai, D. Barlam, R. Z. Shneck, E. Gazit, I. Rousso, *Angew. Chem.* **2010**, 122, 10135.
- [20] J. M. Gere, *Mechanics of Materials*, 6th ed., Thomson Learning, Inc. Stamford, Connecticut, US **2004**.
- [21] a) A. Almetwally, M. Salem, *Autex Res. J.* **2010**, 10, 35; b) X. Sui, E. Wiesel, H. D. Wagner, *Polymer* **2012**, 53, 5037; c) H. D. Wagner, *J. Polym. Sci., Part B: Polym. Phys.* **1989**, 27, 115; d) H. D. Wagner, *J. Macromol. Sci., Part B* **1989**, 28, 339.
- [22] I. Azuri, L. Adler-Abramovich, E. Gazit, O. Hod, L. Kronik, *J. Am. Chem. Soc.* **2014**, 136, 963.
- [23] I. Azuri, E. Meirzadeh, D. Ehre, S. R. Cohen, A. M. Rappe, M. Lahav, I. Lubomirsky, L. Kronik, *Angew. Chem.* **2015**, 127, 13770; *Angew. Chem., Int. Ed.* **2015**, 54, 13566.
- [24] Y. Le Page, P. Saxe, *Phys. Rev. B* **2002**, 65, 1.
- [25] C. Li, A.-K. Born, T. Schweizer, M. Zenobi-Wong, M. Cerruti, R. Mezzenga, *Adv. Mater.* **2014**, 26, 3207.
- [26] P. Podsiadlo, A. K. Kaushik, E. M. Arruda, A. M. Waas, B. S. Shim, J. Xu, H. Nandivada, B. G. Pumplun, J. Lahann, A. Ramamoorthy, N. A. Kotov, *Science* **2007**, 318, 1.
- [27] Z. Gan, X. Wu, J. Zhang, X. Zhu, P. K. Chu, *Biomacromolecules* **2013**, 14, 2112.